A DENSITY FUNCTIONAL THEORY STUDY BASED ON MONOLIGNOLS: MOLECULAR STRUCTURE, HOMO-LUMO ANALYSIS, MOLECULAR ELECTROSTATIC POTENTIAL

FERIDE AKMAN

University of Bingöl, Vocational School of Technical Sciences, Bingöl 12000, Turkey
✉ *Corresponding author: chemakman@gmail.com*

Received May 15, 2018

In the present study, three monomeric subunits, sinapyl alcohol, coniferyl alcohol and p-coumaryl alcohol, were investigated in terms of chemical shift, vibrational spectroscopic, molecular geometry and quantum chemical calculations. HOMO-LUMO analysis, electronegativity, hardness, electrophilicity index, softness and molecular electrostatic potential (MEP) results were also reported using the density functional theory (DFT/B3LYP) method with 6-31G (d,p) basis set. The computed HOMO and LUMO energies confirmed that charge transfer took place within the monolignols. The positive region of the MEP is associated with nucleophilic reactivity and the negative region – with electrophilic reactivity, as shown in the MEP plots, while the monolignols have various probable regions.

Keywords: lignin, density functional theory (DFT), coniferyl alcohol, p-coumaryl alcohol, sinapyl alcohol

INTRODUCTION

Lignin is the second most abundant terrestrial biopolymer, or renewable natural polymer, after cellulose. It has various properties and applications, *e.g.* as adhesive, binder, fiber nutritional source, dispersing agent, flocculent and thickener in paints and coatings, which can increase its potential value. Lignin also provides defense against pathogens and pests and is very important for both mechanical and vascular transport.[1,2]

Lignin has a complex three-dimensional structure formed by free radical polymerization of three monomeric subunits, *i.e.* sinapyl alcohol, p-coumaryl alcohol and coniferyl alcohol, in plants.[3] These precursors are called monolignols. Based on the type, part and growth environment of the plant, its lignin structure may differ in terms of the amount and type of monomeric subunits.[4,5] For instance, hardwood lignin involves approximately 1:1 (sinapyl:coniferyl alcohol) monomeric units, whereas softwood lignin contains these units in a roughly 1:9 ratio.[6] Moreover, lignin is one of the primary cell wall ingredients in arboreal plants and, after cellulose, it is the best known biopolymer. Apart from its structural function, lignin plays a very important role biologically in plants. Besides, lignin prevents the absorption of water by polysaccharides, as it is much less hydrophilic than hemicelluloses and cellulose. Therefore, knowledge of its chemical structure is as important as that of other natural polymers. In the industry, only a small fraction of the lignin obtained as a waste by-product is used commercially, thus valorizing its various aromatic units, functional groups, conjugated linkages and molecular size.[7] Therefore, a detailed investigation of lignin and its components could provide solutions to the problem. While such a study would be expensive and time-consuming, a theoretical approach will bring both time and cost reducing benefits. The structure and reactivity of lignin can be researched by theoretical methods. Recently, the density functional theory (DFT), which is one of the most important theoretical modeling methods, has been used to predict correctly the structures, as well as the physical and chemical properties of molecules.[8,9]

The aim of this study was to obtain deeper understanding of the three monomeric subunits of lignin using the density functional theory (DFT) method. Density functional theory (DFT) calculations were performed for the monolignols, using the standard 6-31G (d, p) basis set.

The FT-IR and ^{1}H-NMR of the monolignols were determined at the DFT/B3LYP level of the theory using the 6-31G (d, p) basis set. The data calculated for monolignols are very important for providing an insight into molecular analysis and then for the use of lignin in technological applications. Considering the fact that the studies using the DFT method, conducted in the past and present, have been confirmed experimentally, future investigations using this method can provide a great guide to chemists and physicists, without requiring experimental studies.

EXPERIMENTAL

Computational methods

The molecular structures of monolignols in the ground state were optimized, using the Gaussian 09[10] and Gaussview 5.0.9 molecular visualization package program,[11] the hybrid functional and Becke's three parameter functional (B3),[12] combined with the gradient–corrected correlational functional of Lee, Yang and Parr (LYP),[13,14] supplemented with the standard 6-31G (d, p) basis set. The ^{1}H chemical shifts, vibrational frequencies, HOMO-LUMO energies, and molecular electrostatic potential surfaces of monolignols were calculated by the same method.

RESULTS AND DISCUSSION

Molecular geometry

Molecular geometry optimizations of the monolignols were performed by the 6-31G (d, p) basis set and indicated in Figure 1 with a numbering scheme. The minimum self-consistence field energy for sinapyl, coniferyl and p-coumaryl alcohols was found to be -19822.114, -16705.456 and -13589.425, respectively. The geometrical parameters optimized for monolignols are listed in Table 1, along with the atomic labelling indicated in Figure 1. The longest lengths for sinapyl, coniferyl and p-coumaryl alcohols are between the C1–C2, C9–H19 and H14–H19 bond distances and indicate values of 1.5064, 2.7064 and 2.1837 Å, respectively, whereas the shortest lengths are O15–H29, O13–H25 and O11–H21 bond distances and indicate values of 0.9650, 0.9637 and 0.9637 Å, respectively. Comparing bond lengths, the C–H and C–C bond lengths are longer than the O–H bond lengths due to the electronegativity of Oxygen (O). In sinapyl alcohol, one of the largest bond angles is computed as 127.622° and ascribed to C2–C3–C4, while one of the smallest bond angles is computed as 104.9627° and ascribed to O7–C8–H21. In coniferyl alcohol, one of the largest bond angles is computed as 168.273° and ascribed to C11–C9–H19, while one of the smallest bond angles is computed as 72.766° and ascribed to C6–C9–H19. In p-coumaryl alcohol, one of the largest bond angles is computed as 128.064° and ascribed to C2–C3–C4, while one of the smallest bond angles is computed as 106.444° and ascribed to H12–C1–H13.

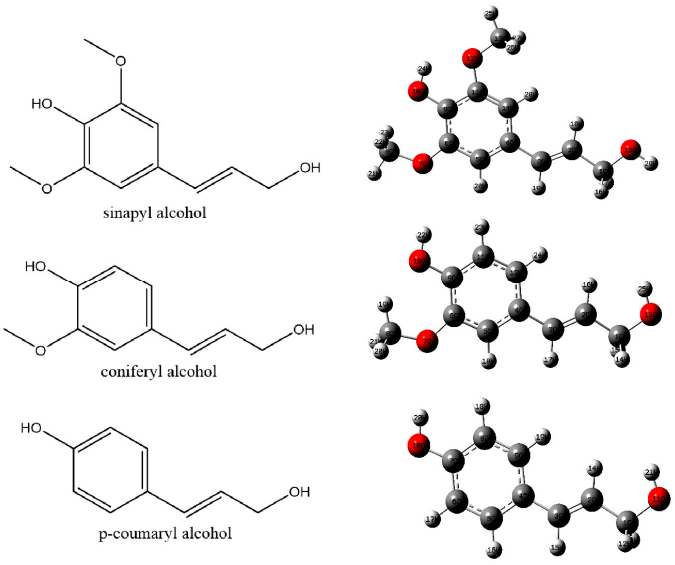

Figure 1: Optimized molecular structure of monolignols

Table 1
Optimized bond lengths (Å), bond angles (°), dihedral angles (°) of monolignols at B3LYP/ 6-31G (d,p) basis set in gaseous phase

Parameters	Sinapyl alcohol	Parameters	Coniferyl alcohol	Parameters	p-Coumaryl alcohol
Bond lengths (Å)					
C1-C2	1.5064	C1-C2	1.5119	C1-C2	1.5115
C1-O15	1.4243	C1-O13	1.4232	C1-O11	1.424
C1-H16	1.1035	C1-H14	1.101	C1-H12	1.1011
C1-H17	1.1035	C1-H15	1.101	C1-H13	1.1011
C2-C3	1.3395	C2-C3	1.3398	C2-C3	1.34
C2-H18	1.0877	C2-H16	1.0916	C2-H14	1.0916
C3-C4	1.4689	C3-C4	1.4691	C3-C4	1.4682
C3-H19	1.0911	C3-H17	1.0909	C3-H15	1.0912
C4-C5	1.3959	C4-C5	1.4002	C4-C5	1.4072
C4-C14	1.4106	C4-C12	1.4054	C4-C9	1.4063
C5-C6	1.4035	C5-C6	1.4011	C5-C6	1.3898
C5-H20	1.0852	C5-H18	1.0857	C5-H16	1.087
C6-O7	1.3656	C6-O7	1.3627	C6-C7	1.398
C6-C9	1.4007	C6-C9	1.411	C6-H17	1.0848
O7-C8	1.4268	O7-C8	1.4306	C7-C8	1.4008
C8-H21	1.092	C8-H19	1.0853	C7-O10	1.3654
C8-H22	1.0933	C8-H20	1.0951	C8-C9	1.39
C8-H23	1.0933	C8-H21	1.0951	C8-H18	1.0882
C9-O10	1.3709	C9-O10	1.377	C9-H19	1.0856
C9-C11	1.4132	C9-C11	1.4004	O10-H20	0.9662
O10-H24	0.9704	C9-H19	2.7064	O11-H21	0.9637
C11-O12	1.3781	O10-H19	2.0545	H14-H19	2.1837
C11-C14	1.385	O10-H22	0.966		
O12-C13	1.4197	C11-C12	1.3869		
C13-H25	1.0909	C11-H23	1.0891		
C13-H26	1.0967	C12-H24	1.0846		
C13-H27	1.0967	O13-H25	0.9637		
C14-H28	1.0821	H16-H24	2.1927		
O15-H29	0.965				
Bond angles (°)					
C2-C1-O15	107.6851	C2-C1-O13	114.06	C2-C1-O11	114.0588
C2-C1-H16	110.2064	C2-C1-H14	109.7407	C2-C1-H12	109.774
C2-C1-H17	110.2065	C2-C1-H15	109.7407	C2-C1-H13	109.774
O15-C1-H16	111.0208	O13-C1-H14	108.278	O11-C1-H12	108.2484
O15-C1-H17	111.0217	O13-C1-H15	108.278	O11-C1-H13	108.2484
H16-C1-H17	106.7235	H14-C1-H15	106.4522	H12-C1-H13	106.444
C1-C2-C3	124.3961	C1-C2-C3	124.4149	C1-C2-C3	124.3921
C1-C2-H18	113.9402	C1-C2-H16	115.8405	C1-C2-H14	115.7999
C3-C2-H18	121.6636	C3-C2-H16	119.7446	C3-C2-H14	119.808
C2-C3-C4	127.6226	C2-C3-C4	127.7489	C2-C3-C4	128.0643
C2-C3-H19	118.1457	C2-C3-H17	117.8309	C2-C3-H15	117.6428
C4-C3-H19	114.2317	C4-C3-H17	114.4201	C4-C3-H15	114.2929
C3-C4-C5	118.7521	C3-C4-C5	118.6744	C3-C4-C5	119.1134
C3-C4-C14	122.7681	C3-C4-C12	123.7858	C3-C4-C9	123.6661
C5-C4-C14	118.4798	C5-C4-C12	117.5399	C5-C4-C9	117.2205
C4-C5-C6	122.6388	C4-C5-C6	123.5677	C4-C5-C6	122.0277
C4-C5-H20	120.5219	C4-C5-H18	120.1614	C4-C5-H16	119.0049
C6-C5-H20	116.8393	C6-C5-H18	116.2709	C6-C5-H16	118.9674
C5-C6-O7	114.3496	C5-C6-O7	113.5002	C5-C6-C7	119.628
C5-C6-C9	118.712	C5-C6-C9	117.8002	C5-C6-H17	121.3416
O7-C6-C9	126.9384	O7-C6-C9	128.6996	C7-C6-H17	119.0304
C6-O7-C8	121.8917	C6-O7-C8	125.67	C6-C7-C8	119.5271
O7-C8-H21	104.9627	O7-C8-H19	113.2437	C6-C7-O10	117.6993
O7-C8-H22	111.8518	O7-C8-H20	107.7553	C8-C7-O10	122.7736
O7-C8-H23	111.8517	O7-C8-H21	107.7553	C7-C8-C9	120.1723
H21-C8-H22	109.6011	H19-C8-H20	109.6561	C7-C8-H18	119.8862
H21-C8-H23	109.6009	H19-C8-H21	109.6561	C9-C8-H18	119.9415
H22-C8-H23	108.8938	H20-C8-H21	108.6545	C4-C9-C8	121.4244
C6-C9-O10	122.733	C6-C9-O10	120.6374	C4-C9-H19	120.0678
C6-C9-C11	118.6084	C6-C9-C11	118.9599	C8-C9-H19	118.5079
O10-C9-C11	118.6586	C6-C9-H19	72.7666	C7-O10-H20	109.1721
C9-O10-H24	105.8754	O10-C9-C11	120.4026	C1-O11-H21	108.5672
C9-C11-O12	112.2267	C11-C9-H19	168.2735	C2-H14-H19	114.1678
C9-C11-C14	122.3739	C9-O10-H22	108.3539	C9-H19-H14	114.226
O12-C11-C14	125.3994	H19-O10-H22	149.3222		

C11-O12-C13	118.2896	C9-C11-C12	122.3225		
O12-C13-H25	106.1966	C9-C11-H23	118.0535		
O12-C13-H26	111.2969	C12-C11-H23	119.624		
O12-C13-H27	111.2968	C4-C12-C11	119.8098		
H25-C13-H26	109.3956	C4-C12-H24	121.0154		
H25-C13-H27	109.3958	C11-C12-H24	119.1748		
H26-C13-H27	109.1962	C1-O13-H25	108.5763		
C4-C14-C11	119.187	C2-H16-H24	114.6406		
C4-C14-H28	120.3706	C8-H19-C9	99.6202		
C11-C14-H28	120.4425	C8-H19-O10	129.4254		
C1-O15-H29	107.9051	C12-H24-H16	113.0646		
		Dihedral angles (°)			
O15-C1-C2-C3	179.9768	O13-C1-C2-C3	180	O11-C1-C2-C3	180
O15-C1-C2-H18	-0.0248	O13-C1-C2-H16	0	O11-C1-C2-H14	0
H16-C1-C2-C3	-58.7883	H14-C1-C2-C3	-58.3226	H12-C1-C2-C3	-58.337
H16-C1-C2-H18	121.2101	H14- C1-C2-H16	121.6774	H12-C1-C2-H14	121.663
H17-C1-C2-C3	58.7408	H15-C1-C2-C3	58.3226	H13-C1-C2-C3	58.337
H17-C1-C2-H18	-121.2608	H15-C1-C2-H16	-121.6774	H13-C1-C2-H14	-121.663
C2-C1-O15-H29	-179.9931	C2-C1-O13-H25	0	C2-C1-O11-H21	0
H16-C1-O15-H29	59.2823	H14-C1-O13-H25	-122.4814	H12-C1-O11-H21	-122.5016
H17-C1-O15-H29	-59.2678	H15-C1-O13-H25	122.4814	H13-C1-O11-H21	122.5016
C1-C2-C3-C4	179.9974	C1-C2-C3-C4	180	C1-C2-C3-C4	180
C1-C2-C3-H19	-0.003	C1-C2-C3-H17	0	C1-C2-C3-H15	0
H18-C2-C3-C4	-9E-4	H16-C2-C3-C4	0	H14-C2-C3-C4	0
H18-C2-C3-H19	179.9987	H16-C2-C3-H17	180	H14-C2-C3-H15	180
C2-C3-C4-C5	179.9973	C1-C2-H16-H24	180	C1-C2-H14-H19	180
C2-C3-C4-C14	-0.0025	C3-C2-H16-H24	0	DC3-C2-H14-H19	0
H19-C3-C4-C5	-0.0024	C2-C3-C4-C5	180	C2-C3-C4-C5	180
H19-C3-C4-C14	179.9978	C2-C3-C4-C12	0	C2-C3-C4-C9	0
C3-C4-C5-C6	-179.9997	H17-C3-C4-C5	0	H15-C3-C4-C5	0
C3-C4-C5-H20	0	H17-C3-C4-C12	180	H15-C3-C4-C9	180
C14-C4-C5-C6	1E-4	C3-C4-C5-C6	180	C3-C4-C5-C6	180
C14-C4-C5-H20	179.9998	C3-C4-C5-H18	0	C3-C4-C5-H16	0
C3-C4-C14-C11	179.9996	C12-C4-C5-C6	0	C9-C4-C5-C6	0
C3-C4-C14-H28	-9E-4	C12-C4-C5-H18	180	C9-C4-C5-H16	180
C5-C4-C14-C11	-2E-4	C3-C4-C12-C11	180	C3-C4-C9-C8	180
C5-C4-C14-H28	179.9994	C3-C4-C12-H24	0	C3-C4-C9-H19	0
C4-C5-C6-O7	-179.9998	C5-C4-C12-C11	0	C5-C4-C9-C8	0
C4-C5-C6-C9	-2E-4	C5-C4-C12-H24	180	C5-C4-C9-H19	180
H20-C5-C6-O7	5E-4	C4-C5-C6-O7	180	C4-C5-C6-C7	0
H20-C5-C6-C9	-179.9999	C4-C5-C6-C9	0	C4-C5-C6-H17	180
C5-C6-O7-C8	-179.9912	H18-C5-C6-O7	0	H16-C5-C6-C7	180
C9-C6-O7-C8	0.0092	H18-C5-C6-C9	180	H16-C5-C6-H17	0
C5-C6-C9-O10	-179.9992	C5-C6-O7-C8	180	C5-C6-C7-C8	0
C5-C6-C9-C11	3E-4	C9-C6-O7-C8	0	C5-C6-C7-O10	180
O7-C6-C9-O10	3E-4	C5-C6-C9-O10	180	H17-C6-C7-C8	180
O7-C6-C9-C11	179.9998	C5-C6-C9-C11	0	H17-C6-C7-O10	0
C6-O7-C8-H21	179.995	C5-C6-C9-H19	180	C6-C7-C8-C9	0
C6-O7-C8-H22	-61.2348	O7-C6-C9-O10	0	C6-C7-C8-H18	180
C6-O7-C8-H23	61.225	O7-C6-C9-C11	180	O10-C7-C8-C9	180
C6-C9-O10-H24	-179.9992	O7-C6-C9-H19	0	O10-C7-C8-H18	0
C11-C9-O10-H24	0.0012	C6-O7-C8-H19	0	C6-C7-O10-H20	180
C6-C9-C11-O12	-179.9993	C6-O7-C8-H20	-121.4615	C8-C7-O10-H20	0
C6-C9-C11-C14	-4E-4	C6-O7-C8-H21	121.4615	C7-C8-C9-C4	0
O10-C9-C11-O12	2E-4	O7-C8-H19-C9	0	C7-C8-C9-H19	180
O10-C9-C11-C14	179.9992	O7-C8-H19-O10	0	H18-C8-C9-C4	180
C9-C11-O12-C13	-179.995	H20-C8-H19-C9	120.3871	H18-C8-C9-H19	0
C14-C11-O12-C13	0.0061	H20-C8-H19-O10	120.3871	C4-C9-H19-H14	0
C9-C11-C14-C4	3E-4	H21-C8-H19-C9	-120.3871	C8-C9-H19-H14	180
C9-C11-C14-H28	-179.9992	H21-C8-H19-O10	-120.3871	C2-H14-H19-C9	0
O12-C11-C14-C4	179.9991	C6-C9-O10-H22	180		
O12-C11-C14-H28	-4E-4	C11-C9-O10-H22	0		
D(C11-O12-C13-H25)	179.9958	C6-C9-C11-C12	0		
C11-O12-C13-H26	-61.0317	C6-C9-C11-H23	180		
C11-O12-C13-H27	61.0231	O10-C9-C11-C12	180		
		O10-C9-C11-H23	0		
		H19-C9-C11-C12	180		
		H19-C9-C11-H23	0		
		C6-C9-H19-C8	0		
		C11-C9-H19-C8	180		
		H22-O10-H19-C8	180		
		C9-C11-C12-C4	0		
		C9-C11-C12-H24	180		
		H23-C11-C12-C4	180		

H23-C11-C12-H24	0
C4-C12-H24-H16	0
C11-C12-H24-H16	180
C2-H16-H24-C12	0

Vibrational frequencies

The vibrational frequencies for the monolignols were computed by the DFT method with the 6-31G (d, p) basis set. The theoretical Fourier transform infrared spectra of sinapyl, coniferyl and p-coumaryl alcohols are illustrated in Figure 2, respectively. The aromatic C–H stretching vibrations are generally found in the region of 3100-3000 cm^{-1}.[15] The vibrations related to the aromatic C–H stretching for sinapyl, coniferyl and p-coumaryl alcohols were computed by the DFT in the vicinity of 3079-3105 cm^{-1}, 3030-3082 cm^{-1} and 3040-3089 cm^{-1}, respectively. The O–H stretching vibrations are generally found in the region of 3400-3600 cm^{-1}.[16] The O–H stretching vibrations bound to the aromatic ring were computed in the vicinity of 3607, 3673 and 3674 cm^{-1}, while the O–H stretching vibrations bound to the ethylene group were calculated to be located in the vicinity of 3684, 3698 and 3699 cm^{-1}, respectively. The vibrations of =C–H stretching were calculated to lie in the regions of 3008-3055 cm^{-1}, 3004-3013 cm^{-1} and 3001-3009 cm^{-1}, respectively. The calculated aliphatic C=C stretching vibrations were found at 1662, 1658 and 1654 cm^{-1}, while the calculated aromatic C=C stretching vibrations were found around 1489-1594, 1501-1598 and 1500-1606 cm^{-1}, respectively.

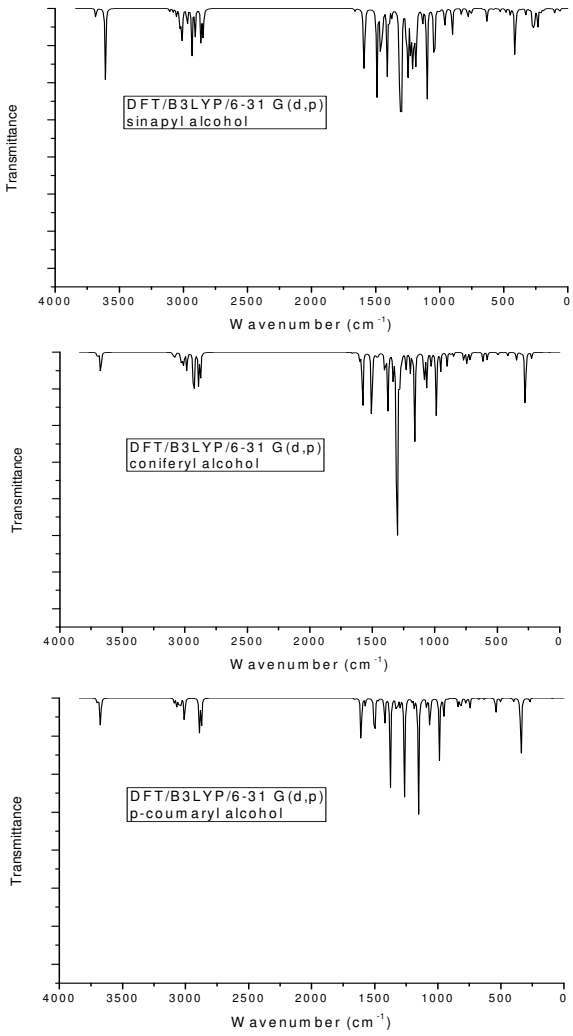

Figure 2: Calculated vibrational frequencies of monolignols

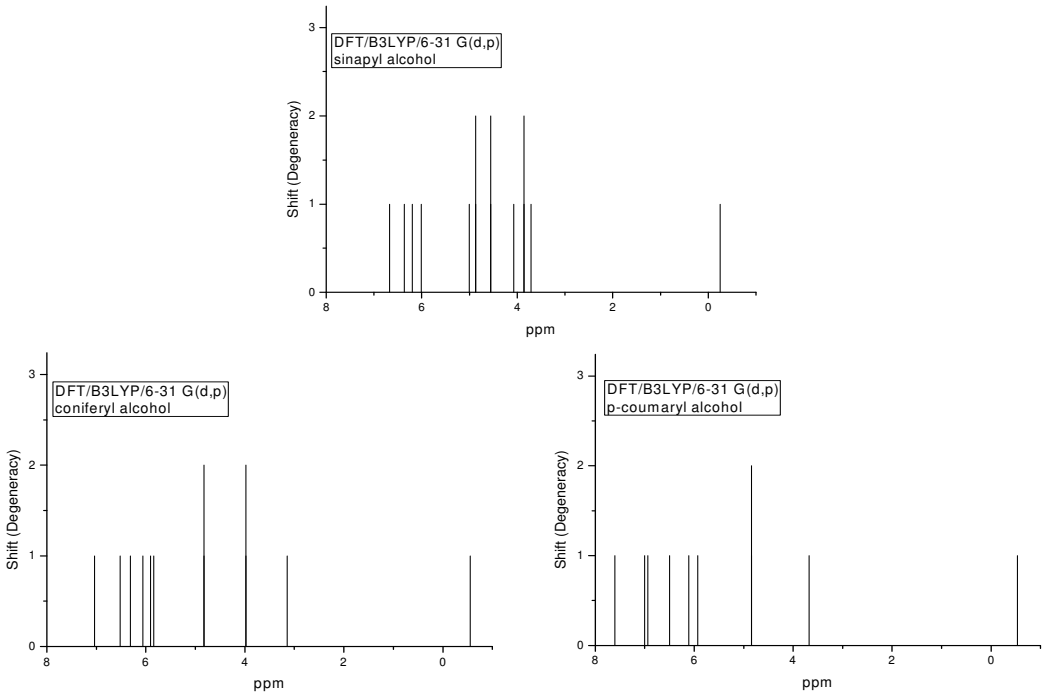

Figure 3: Calculated ^{1}H-NMR of monolignols

The aromatic ring C=C stretching vibrations mostly indicate the region of 1625-1400 cm^{-1}.[17] The values computed for the C=C stretching signals are in accordance with the experimental values in the literature. Besides, the bands at 1465, 1469 and 1469 cm^{-1} are due to the signal of CH_2, next to the ethylene and hydroxyl group. As a result, the theoretical results are compatible with each other.

NMR analysis

The theoretical ^{1}H-NMR spectra of the monolignols are indicated in Figure 3. The theoretical ^{1}H-NMR spectra of sinapyl, coniferyl and p-coumaryl alcohols show characteristic signals at 6.20-6.68 ppm, 6.31-7.04 and 6.50-7.61 ppm, which are ascribed to aromatic ring protons, respectively. The signals at 5.01, 3.14 and 3.68 ppm are ascribed to –OH protons bound to the aromatic ring, respectively; while the signals at 6.01 and 6.37, 5.91 and 6.06, 5.93 and 6.11 ppm are ascribed to ethylene protons, respectively. Besides, in sinapyl alcohol, the signals at 3.71-4.56 ppm are ascribed to the protons of methoxy groups bound to the aromatic ring, the signals at 4.87 ppm are ascribed to $–CH_2$ protons adjacent to hydroxyl and ethylene groups. In coniferyl alcohol, the signals at 3.97-5.84 ppm are ascribed to the protons of methoxy groups bound to the aromatic ring, the signals at 4.82 ppm are ascribed to $–CH_2$ protons adjacent to hydroxyl and ethylene groups. In p-coumaryl alcohol, the signals at 4.84 ppm are ascribed to $–CH_2$ protons adjacent to hydroxyl and ethylene groups. The signals in the region between 8.00 and 7.00 ppm are generally ascribed to the chemical shift of aromatic protons. As a result, the theoretical results are compatible with each other.

Frontier molecular orbitals

LUMO stands for the lowest unoccupied molecular orbital, and HOMO stands for the highest occupied molecular orbital; they are also called FMOs (frontier molecular orbitals). While LUMO acts as an electron acceptor, HOMO acts as an electron donor. The 3D plots of LUMO and HOMO for the monolignols are exhibited in Figure 4. The electronegativity (χ), electron affinity (A), chemical hardness (η), ionization potential (I), chemical potential (μ_o), softness (ς) and electrophilicity index (ω) were calculated with the help of the energy gap between HOMO-LUMO, using the B3LYP/6-31G (d, p) basis set,[18] and the values are listed in Table 2.

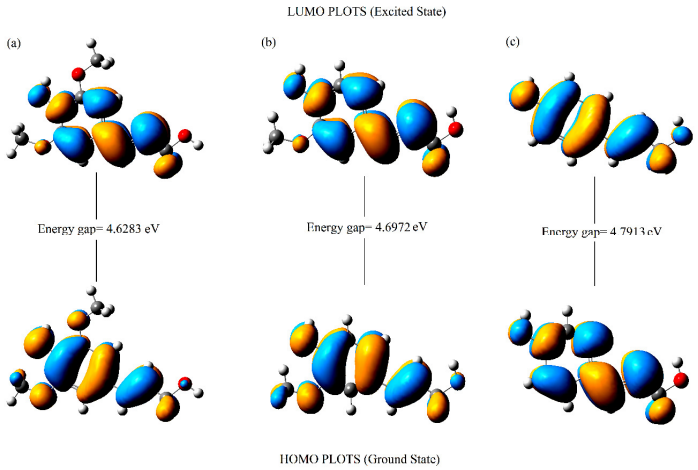

Figure 4: Frontier molecular orbitals (FMOs) of sinapyl alcohol (a), coniferyl alcohol (b) and p-coumaryl alcohol (c)

Table 2
Some electronic properties for monolignols at B3LYP/6-31G (d, p) basis set in gaseous phase

Parameters (eV)	Sinapyl alcohol	Coniferyl alcohol	p-Coumaryl alcohol
E_{HOMO}	-5.075	-5.360	-5.560
E_{LUMO}	-0.447	-0.663	-0.769
Energy band gap [$\Delta E = E_{LUMO} - E_{HOMO}$]	4.628	4.697	4.791
Electrophilicity index (ω)	1.647	1.930	2.089
Softness (ς)	0.432	0.425	0.417
Ionization energy (I)	5.075	5.360	5.560
Chemical potential (μ_o)	2.761	3.011	3.164
Dipole moment (μ)	1.537 Debye	3.776 Debye	2.538 Debye
Electron affinity (A)	0.447	0.663	0.769
Electronegativity(χ)	-2.761	-3.011	-3.164
Chemical hardness (η)	2.314	2.348	2.395
SCF energy	-19822.114	-16705.456	-13589.425

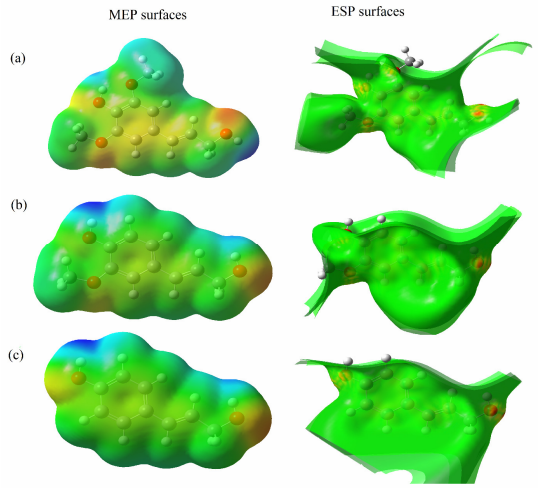

Figure 5: MEP and ESP surfaces of sinapyl alcohol (a), coniferyl alcohol (b) and p-coumaryl alcohol (c)

If the energy gap between HOMO and LUMO is small, then the molecule is associated with high polarisability, low kinetic stability and high chemical reactivity.[19] In the sinapyl, coniferyl and p-coumaryl alcohols, the value of the HOMO-LUMO energy gap was found to be 4.62, 4.69 and

4.79 eV, respectively, demonstrating that charge transfer occurs to a greater extent within sinapyl alcohols.

Molecular electrostatic potential analysis

Molecular electrostatic potential (MEP) maps show the electron density of the molecules three dimensionally and serve as very important descriptors for nucleophilic and electrophilic attack regions and hydrogen bonding interactions.[20,21] Analysis of MEP surfaces was performed by using the same basis set to determine the reactive regions of nucleophilic and electrophilic attack for the monolignols and the results are illustrated in Figure 5. The different colors on the MEP surfaces are the result of different values of electrostatic potential. Potential values decrease in the order of blue>green>yellow>orange>red. The negative region of MEP (red coded region), which is related to electrophilic reactivity, covers the hydroxyl groups due to the oxygen atoms, while the positive region (blue coded region), which is related to nucleophilic reactivity, covers the hydrogen atoms. The higher electronegativity in the hydroxyl groups makes it the most reactive part in the monolignols. The electrostatic potential (ESP) surfaces of monolignols are indicated in Figure 5. The partial charges and electronegativity of the atoms affect the electrostatic potential values. Therefore, the negative ESP is localized more around the oxygen atoms (seen as a reddish blob), whereas the positive ESP is localized on the rest of the monolignols.

CONCLUSION

In the present study, sinapyl alcohol, p-coumaryl alcohol and coniferyl alcohol were researched theoretically. Firstly, the molecular geometries and molecular structural parameters of the monolignols were determined using the density functional theory (DFT/B3LYP) method, with 6-31G (d, p) basis set. Secondly, the scaled vibrational frequencies and the chemical shifts of the monolignols were calculated using the same method. Finally, the analysis of the MEP surfaces was performed to determine the reactive regions and the energy gap between LUMO and HOMO was computed. We hope that this study will be useful to the researchers who are in quest of theoretical and experimental evidence related to the use of monolignols in various materials and applications. Because earlier studies conducted by the DFT method have been confirmed experimentally, future computation using this method can serve as a great tool to scientists.

ACKNOWLEDGEMENTS: The author wishes to thank the Scientific and Technological Application and Research Center of Bingöl University, and Bitlis Eren University for providing the Gaussian software.

REFERENCES

[1] B. M. Upton and A. M. Kasko, *Chem. Rev.*, **116**, 2275 (2016), https://doi.org/10.1021/acs.chemrev.5b00345
[2] K. V. Sarkanen and C. H. Ludwig, "Lignins: Occurrence, Formation, Structure and Reactions", Wiley-Interscience, 1971.
[3] A. E. Harman-Ware, M. Crocker, A. P. Kaur, M. S. Meier, D. Kato *et al*., *J. Anal. Appl. Pyrol*., **99**, 161 (2013), https://doi.org/10.1016/j.jaap.2012.10.001
[4] D. G. J. Mann, N. L. Labbe, R. W. Sykes, K. Gracom, L. Kline *et al*., *Bioenerg. Res*., **2**, 246 (2009), https://doi.org/10.1007/s12155-009-9054-x
[5] J. R. Obst, *Holzforschung*, **36**, 143 (1982), https://doi.org/10.1515/hfsg.1982.36.3.143
[6] J. Zakzeski, P. C. A. Bruijnincx, A. L. Jongerius and B. M. Weckhuysen, *Chem. Rev*., **110**, 3552 (2010), https://doi.org/10.1021/cr900354u
[7] D. Huber, A. Ortner, A. Daxbacher, G. S. Nyanhongo, W. Bauer *et al*., *ACS Sustain. Chem. Eng*., **4**, 5303 (2016), 10.1021/acssuschemeng.6b00692
[8] F. Akman, *Polym. Bull*., **74**, 2975 (2017), DOI: 10.1007/s00289-016-1875-0
[9] F. Akman, *Can. J. Phys*., **94**, 853 (2016), https://doi.org/10.1139/cjp-2016-0252
[10] M. J. Frisch, G. W. Trucks, H. B. Schlegel, G. E. Scuseria, M. A. Robb *et al*., Gaussian 09, Gaussian Inc., Wallingford CT, 2010.
[11] R. Dennington, T. Keith and J. Millam, GaussView, Version 5, Semichem Inc., Shawnee Mission KS, 2010.
[12] A. D. Becke, *Phys. Rev. A*, **38**, 3098 (1988), https://doi.org/10.1103/PhysRevA.38.3098
[13] C. Lee, W. Yang and R. G. Parr, *Phys. Rev. B*, **37**, 785 (1988), https://doi.org/10.1103/PhysRevB.37.785
[14] A. D. Becke, *J. Chem. Phys*., **98**, 5648 (1993), https://doi.org/10.1063/1.464304
[15] G. Varsanyi, "Assignments for Vibrational Spectra of Seven Hundred Benzene Derivatives", vol. 1, Adam Hilger, London, 1974.
[16] R. M. Silverstein and F. X. Webster, "Spectroscopic Identification of Organic Compounds", sixth ed., John Willey and Sons, New York, 1998.
[17] V. Krishnakumar, N. Surumbarkuzhali and S. Muthunatesan, *Spectrochim. Acta A*, **71**, 1810 (2009).
[18] F. Akman, *Cellulose Chem. Technol*., **51**, 253 (2017), http://www.cellulosechemtechnol.ro/pdf/CCT3-4(2017)/p.253-262.pdf

[19] I. Fleming, "Frontier Orbital and Organic Chemical Reactions", John Wiley and Sons, New York, 1976.
[20] E. Scrocco and J. Tomasi, *Adv. Quantum. Chem.*, **103**, 115 (1978), https://doi.org/10.1016/S0065-3276(08)60236-1
[21] F. J. Luque, J. M. Lopez and M. Orozco, *Theor. Chem. Acc.*, **103**, 343 (2000), https://doi.org/10.1007/s002149900013